Hindawi
Discrete Dynamics in Nature and Society
Volume 2022, Article ID 7848008, 7 pages
https://doi.org/10.1155/2022/7848008

*Research Article*

# Signal Analysis of Characteristics Using Passive Acoustic Emission Technique in Gas-Solid Pipeline Flows

**Weigang Qin**

*School of Electronic and Information Engineering, Tiangong University, Tianjin 300387, China*

Correspondence should be addressed to Weigang Qin; qinweigang@tiangong.edu.cn

Received 25 April 2022; Accepted 7 June 2022; Published 29 June 2022

Academic Editor: Zi-Peng Wang



This paper investigates a case study of the use of a passive acoustic sensor for online measurement of the dilute phase gas-solid pipeline flows. The acoustic emission sensor is mounted externally on a stainless steel line conveying silica powders. For different experimental conditions, including the solid to air mass ratios from 0.6 to 1.4 and the gas volume flows from 160 to 240 $m^3/h$, the sound signals in the pipeline are discussed using the wavelet transform technique. The measured values of transmission mechanism of two different lengths, 25 mm and 35 mm, are analyzed. The results show that the variation tendency of standard deviations is consistent and that the noninvasive, online acoustic detect technique can be regarded as a satisfactory tool in gas-solid flows.

## 1. Introduction

Pneumatic conveying is commonly referred to wind power transport of granular materials with a certain air pressure and speed in industry. Pneumatic conveying is widely used in different fields, such as grain, cement, coal, chemical materials, powder, salt, flour, and other industrial processes.

There are many methods to measure gas-solid two-phase flow, such as the microwave method [1], electrostatic method [2], electrical tomography [3], optical method [4], and acoustic method [5]. Previous work is encountered in the technique using acoustic signals to measure particle size and other characteristics in dilute phase pneumatic conveying lines. The electrostatic method and image method are conducted in gas-solid flow regimes. For instance, the electrostatic method is adapted for electrostatic correlation velocimetry, while the image method is used in the movement of particles and flames imaging. The work has also demonstrated the feasibility of using acoustic measurement of particle size by Yan [6]. The active acoustic technique in gas-solid two-phase flows has been studied in different locations near the pipeline bends to measure the flow velocity and particle concentration. The results show that the speed near the elbow is divergent from one of the straight pipes and that the concentration at the elbow is approximately twice in the straight pipe [7]. Dilute phase flow has been observed in the pneumatic transport of fine powders. As the gas flow rate is reduced or the solids flow rate increased, particles may settle on the bottle of the horizontal sections, forming a stagnant layer, and affecting the stability of the fluid. Therefore, the work is to develop reliable flow regime detection through the online analysis of signals reflecting the solid phase velocity from nonintrusive acoustic sensors [8, 9]. Particle size is inferred from measurement of the peak compression of a specially designed ultrasonic transducer subject to the impact of the particles using a noninvasive acoustic sensor. In the laboratory, the impact size monitor (ISM) has demonstrated the ability to discriminate between powders with a difference in peak particle size of 2% at an approximate peak size of 150 microns [10]. Acoustic method, determining the pipeline leak location, also shows that the technique can achieve the online measurements [11]. With discussing the relationship between acoustic signals and particle size distribution, signal processing technique based on acoustic emission is used to extract the sound signal through the wavelet transform, thus multivariate dimension is reduced through component analysis. Finally, particle size distribution is obtained in terms of

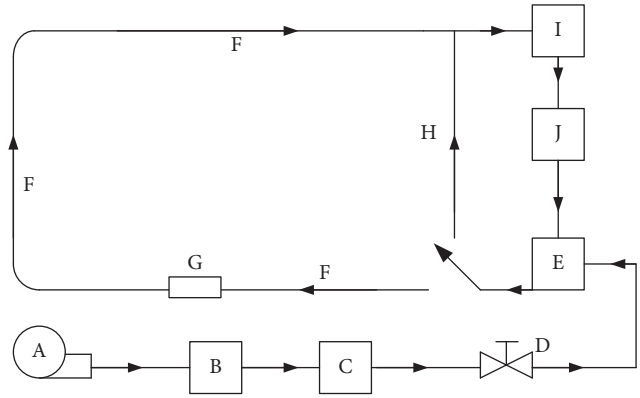


Figure 1: Schematic diagram of the experimental system: A: air compressor, B: gas tank, C: air dryer, D: regulating valve, E: screw feeder, F: transport pipeline, G: acoustic sensor, H: removing blockage pipeline, I: solid storage silo, and J: weighing device.

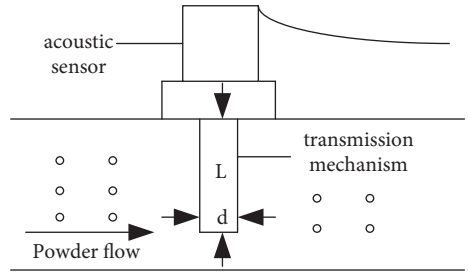


Figure 2: Schematic diagram showing the layout of acoustic sensor.

neural networks [12]. A quantitative model is established to detect related process parameters, including particle concentration, volume flow, and mass flow using passive acoustic sensors [13, 14]. Online measurement signals are achieved through passive acoustic emission sensors used in chemical process. Because of the particle collision, sound frequency between 15 kHz and 200 kHz is described [15]. Combined with the particle temperature and particle collision mechanism, the quality of the gas-solid fluidized bed is judged by signal analysis [16]. Ultrasonic waves are applied to improve the gas-solid flow homogeneity in CFB risers. The best geometrical configuration of an ultrasonic device with a frequency of 40 kHz applied to a lab-scale CFB riser is defined with a design of experiments [17].

The mechanism of acoustic emission in gas-solid flows mainly comes from three aspects: collision between the particles the wall or pipeline, and fluid turbulence. Since the frequency below 20 kHz is difficultly absorbed into the solid, internal ultrasonic sound generated by particles' friction and collision with the wall is detected through the passive acoustic detection systems. The acoustic method combined with principal component analysis, neural network analysis, and wavelet analysis, is widely used in the measurement of gas-solid two-phase flow parameters [18, 19].

## 2. Basic Principles

When extracting the spectrum of the signal, the Fourier transform needs to use the time-domain information of the signal. The time when the frequency component

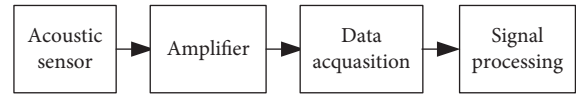


Figure 3: Whole signal processing system.

contained in the signal appears is uncertain. Compared with Fourier transform, wavelet transform converts the infinite trigonometric function basis in Fourier transform into a finite attenuated wavelet basis and analyzes the signal with a set of basic functions with changing width. Therefore, wavelet transform can not only obtain the frequency but also locate the time. Wavelet analysis is also a rapidly developing new field in signal analysis and has been widely used.

*2.1. Continuous Wavelet Transform in Time Domain.* For function,

$$W_s(t) = a^{-1/2} \int_{-\infty}^{+\infty} s(t)\psi_{a,b}^*\left(\frac{t-b}{a}\right)\mathrm{d}t, \tag{1}$$

we further obtain

$$W_s(t) = \int_{-\infty}^{+\infty} s(t)\psi_{a,b}^*(t)\mathrm{d}t = \langle s(t), \psi_{a,b}(t)\rangle, \tag{2}$$

where $s(t)$ represents the signal, $\varphi_{a,b}(t) = \psi_{a,b}(t) = a^{-1/2}\varphi_{a,b}(t - b/a)$ is the kernel function, which is the result of the scaling a and time translation $b$ of the window function. The window function $\psi(t)$ is called the

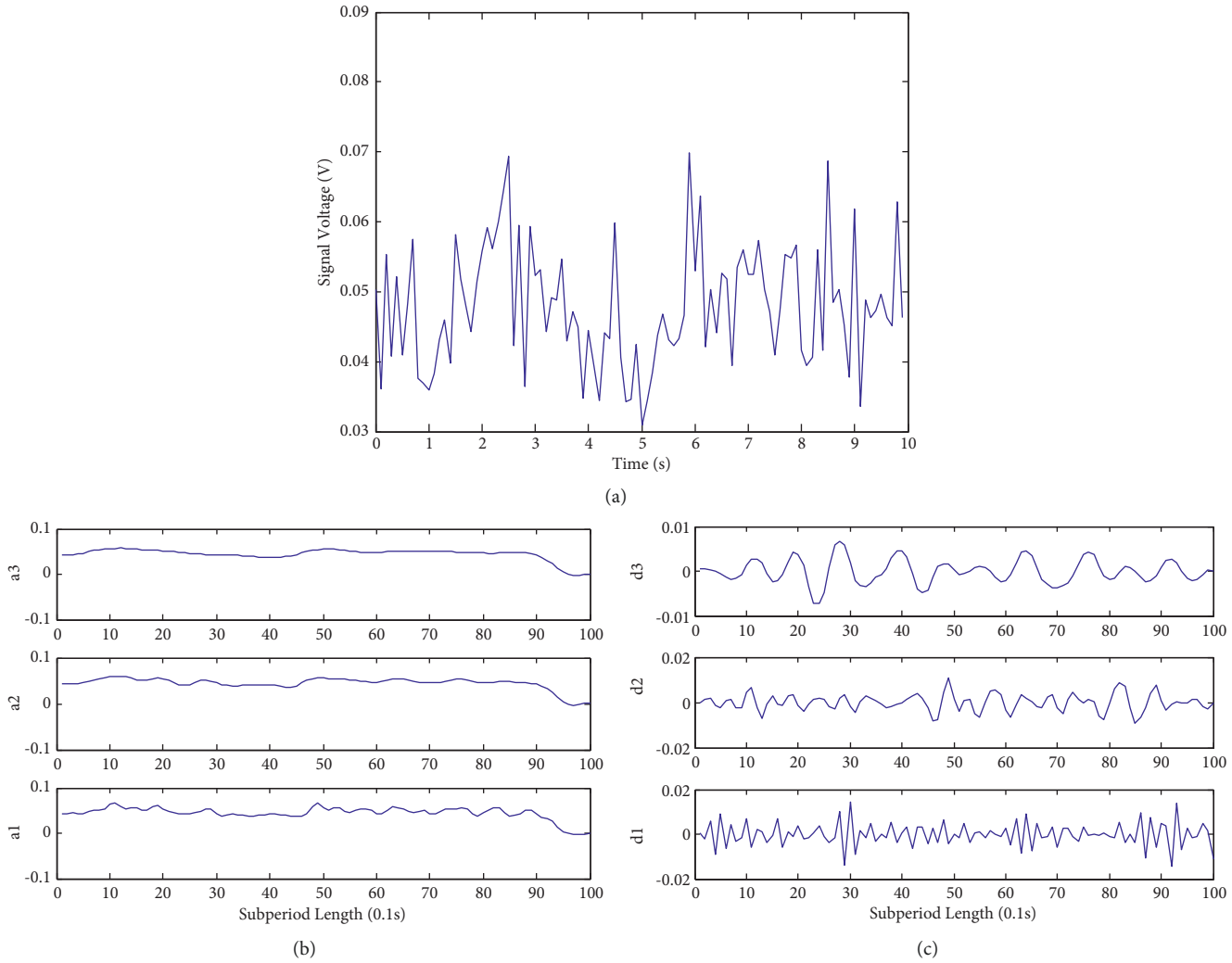


FIGURE 4: (a) FFT signal with solid to air mass ratio 0.6 and gas flow of 160 $m^3$/h; (b) wavelet transform approximation signal; (c) wavelet transform detail signal.

mother wavelet, where $a > 0$ is the scaling of the basic wavelet. $B \in R$ is the time position of the analysis signal, that is, the time center. It is to ensure that the energy of the function and the mother wavelet is the same under different scales [20–22].

*2.2. Wavelet Transform in Frequency Domain.* For function,

$$W_s(\omega) = \frac{a^{1/2}\int_{-\infty}^{+\infty} S(\omega)\widehat{\psi}^*(a\omega)e^{j\omega b}\mathrm{d}\omega}{2\pi} = \frac{\langle S(\omega), \widehat{\psi}_{a,b}(\omega)\rangle}{2\pi},$$
$$\widehat{\psi}_{a,b}(\omega) = a^{-1/2}\widehat{\psi}(a\omega)e^{-j\omega b}, \tag{3}$$

where $S(\omega)$ represents the frequency domain transformation of $s(t)$ and $\widehat{\psi}(\omega)$ is the frequency transformation of $\psi(t)$.

## 3. Experimental System

*3.1. Pneumatic Transport System.* The pneumatic transport circuit is shown schematically in Figure 1. The loop consists of 0.5 m inside diameter stainless steel pipeline. Air is supplied by two compressors, regulated using a valve and monitored by several pressure gauges. Air flows through a horizontal pipeline located underneath a gas-solid mixer from which particles are fed into the pipeline with a weighing device. After the powder feeds point, the gas-solid mixture flows through a 6 m horizontal line with five 6 m horizontal sections and a 3 m vertical line into powder hopper and a cyclone where particles are separated from the air. The gas stream is controlled by a regulating valve. The amount of particles in the loop is determined by a weighing device. In order to avoid solid blockage, it is necessary to use a removing blockage pipeline connecting a cyclone.

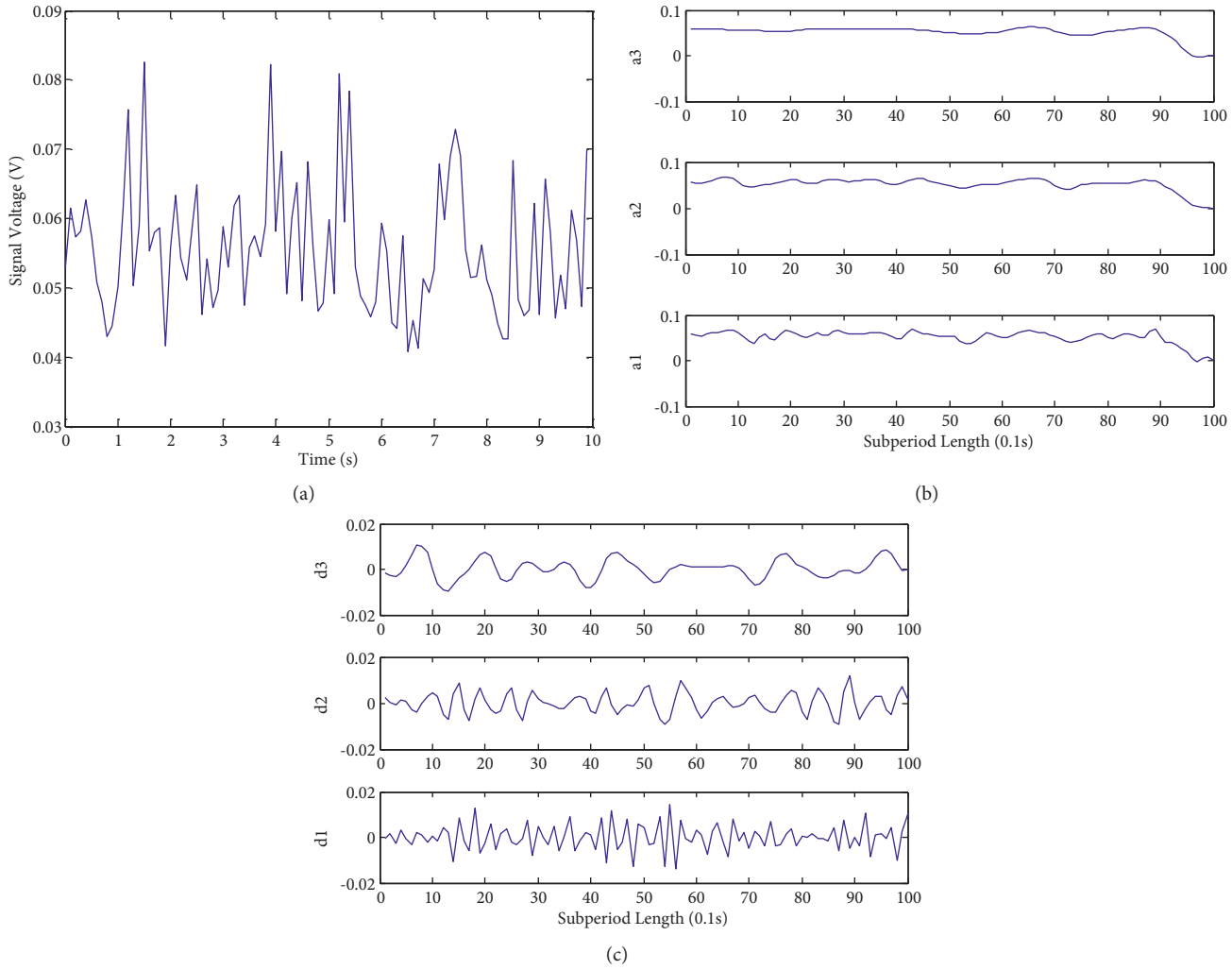


Figure 5: (a) FFT signal with solid to air mass ratio 1.0 and gas flow of 160 $m^3$/h; (b) wavelet transform approximation signal; (c) wavelet transform detail signal.

*3.2. Particle Properties.* Silica particles with white powder, the density of 2.65 g/$cm^3$, the diameter of 100 um, are used in the whole experiment. Its physical properties cannot be changed with high hardness, moisture-proof performance, and easily saving under experimental conditions.

*3.3. Measurement System.* Acoustic sensors can provide a reliable, online, and nonintrusive monitoring. There are two acoustic monitoring methods, that is, active acoustics and passive acoustics [8].

As we all know, the direct impact of particles on the object's surface will cause the rebound of particles, and the rebound particles and subsequent particles will cause secondary or multiple impacts. To reduce multiple bounce caused by particle collision, as shown in Figure 2, the sound transmission device is a stainless steel rod with the particles hitting its diamond-shaped surface. The $d$ is the diagonal of the diamond-shaped surface and $L$ is the length of the device. The diagonal width $d$ with 10 mm and two kinds of length $L$ with 25 mm and 35 mm are selected here. The acoustic emission sensor is installed externally on a horizontal pipe (shown in Figure 1). This position is also where the particles are fully mixed. In order to better measure the sound of particles, the viscous couplant is located between the sound transmission device and the acoustic sensor.

## 4. Experimental Results and Discussion

For each experiment, the different solid to air mass ratios depending on the motor speed are 0.6, 1.0, and 1.4. Whereas for air, the stable gas fluxes are 160, 200, and 240 $m^3$/h. The measuring signals are acquired from the rod of two different lengths of 25 mm and 35 mm.

Firstly, solids are not added to the pneumatic pipeline until the gas flow into the line reaches a stable condition for some time. Once the air flow stabilized, acoustic measurements are recorded right away. After each measurement, the powder hopper is stopped and the gas maintained in the process until the line is completely cleared of solids.

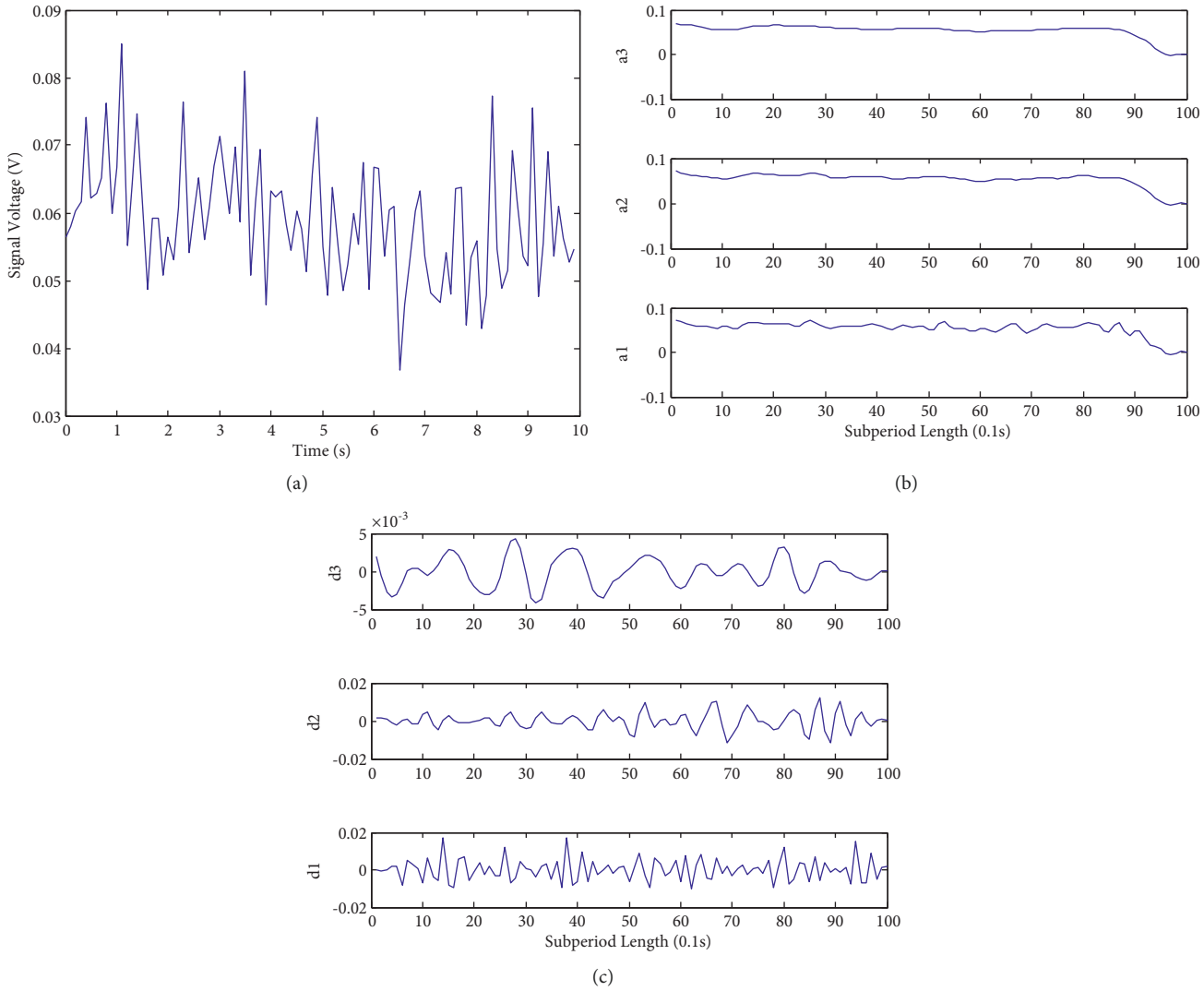


FIGURE 6: (a) FFT signal with solid to air mass ratio 1.4 and gas flow of 160 $m^3$/h; (b) wavelet transform approximation signal; (c) wavelet transform detail signal.

All measurements in the laboratory are performed with commercially available instrumentation and sensors. The whole signal processing system is given in Figure 3. The signal of acoustic emission sensor manufactured by the PengXiang Technology Co., Ltd. is collected and then magnified in the experiment. Finally, the signal is fed into the personal computer using NI Labview USB6259 acquisition card. In addition, according to Shannon sampling theorem, if the maximum signal frequency is $f_m$, then the sampling frequency $f$ must meet $f \geq 2\ f_m$. As the frequency band of the acoustic sensor in the work is 15–165 kHz, the sampling rate of 1 MHz and the acquisition time of 10 s are set to record detail spectral characteristics of the signal in frequency domain.

Figures 4(a), 5(a), and 6(a) show that the 105 acquisition points within every 0.1 s for the fast Fourier transform (FFT) are carried out 100 times for the rod of length 35 mm. The Daubechies3 wavelet approximation signals are obtained in Figures 4(b), 5(b), and 6(b). Figures 4(c), 5(c), and 6(c) represent the Daubechies3 wavelet detail signals, respectively.

Figures 4(a), 5(a), and 6(a) show the signal voltage of acoustic measurement recorded at the different solid to air mass ratios: 0.6, 1.0, and 1.4, after the FFT, filtered to eliminate the 50 Hz electrical noise. With the solid to air mass ratio increasing, the signal voltage magnitude is significantly strengthened. The wavelet transform approximation signals and detail signals are demonstrated in figures 4(b), 4(c), 5(b), 5(c), 6(b), and 6(c).

With the solid to air mass ratio increasing, under the different gas volume flows, the standard deviation of measurement signal is summarized in Figure 7. Under the same gas volume flow and the different solid to air mass ratios, the standard deviation is increased. Meanwhile, under the different gas volume flows and the same solid to air mass ratio, the standard deviation is also increased. Whether the rod length is 25 mm or 35 mm, the trend of standard deviation is

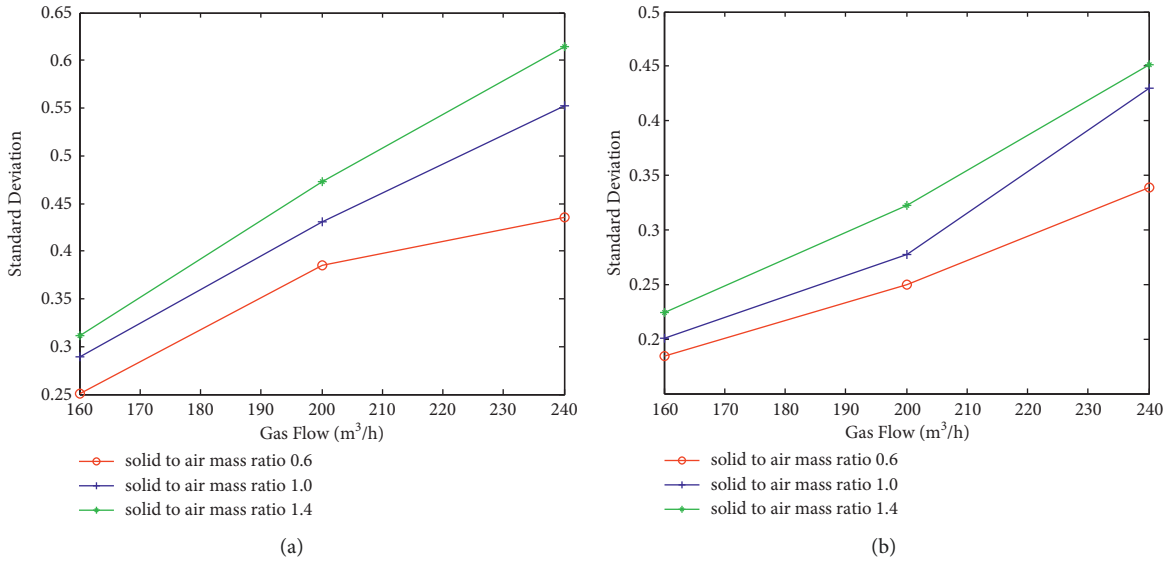


Figure 7: (a) Standard deviation of rod length 25 mm for different gas volume flows and different solid to air mass ratios; (b) standard deviation of rod length 35 mm for different gas volume flows and different solid to air mass ratios.

Table 1: Standard deviation of different lengths.

| Length of rod (mm) | Solid to air mass ratio | Gas volume flow ($m^3$/h) | Standard deviation |
|---|---|---|---|
| 25 | 0.6 | 160 | 0.1838 |
| | | 200 | 0.2495 |
| | | 240 | 0.3385 |
| | 1.0 | 160 | 0.2010 |
| | | 200 | 0.2775 |
| | | 240 | 0.4300 |
| | 1.4 | 160 | 0.2242 |
| | | 200 | 0.3222 |
| | | 240 | 0.4510 |
| 35 | 0.6 | 160 | 0.2501 |
| | | 200 | 0.3855 |
| | | 240 | 0.4350 |
| | 1.0 | 160 | 0.2891 |
| | | 200 | 0.4305 |
| | | 240 | 0.5523 |
| | 1.4 | 160 | 0.3114 |
| | | 200 | 0.4732 |
| | | 240 | 0.6142 |

basically consistent. The standard deviation for every case is shown in Table 1.

## 5. Conclusions

The passive acoustic measurement apparatus described in this experiment operates in the dilute phase gas-solid flows following the horizontal pipeline. The acquisition points are analyzed to obtain approximation signals and detail signals using wavelet transform method. The results present that the collision chance is increased by the different solid to air mass ratios from 0.6 to 1.4 and the same gas volume flow. However, under the same solid to air mass ratio and the different gas volume flows from 160 to 240 $m^3$/h, the signals obtained from the acoustic sensor are enhanced as the more impact between the particles and sound transmission device in the pipeline. At the same time, the standard deviation is obviously increased under the different gas volume flow and the different solid to air mass ratios. The longer the length of the transmission mechanism is, the bigger the standard deviation is. The standard deviation is roughly proportional to the solid to air mass ratio and the gas volume flow, but their value can be acceptable. It is confident that the passive acoustic measurement will bring major improvements to gather the characteristics of gas-solid regime in this study. The relationship between gas flow rate and particle size concentration is established. The advantage of acoustic method is that it is not affected by static electricity. This method is suitable for the measurement of gas-solid two-phase flow. At the same time, a lot of work needs to be done in the future, such as multisensor data fusion technology.

## Data Availability

The data used to support the findings of this study are available from the author upon request.

## Conflicts of Interest

The author declares that there are no conflicts of interest.

## Acknowledgments

The work was supported by the collaborative education project of industry university cooperation of the Ministry of Education (201901138036).

## References

[1] J. Zou, C. Liu, H. Wang, and Z. Wu, "Mass flow rate measurement of bulk solids based on microwave tomography and microwave Doppler methods," *Powder Technology*, vol. 360, pp. 112–119, 2020.

[2] M. Manafi, R. Zarghami, and N. Mostoufi, "Effect of electrostatic charge of particles on hydrodynamics of gas-solid fluidized beds," *Advanced Powder Technology*, vol. 30, no. 4, pp. 815–828, 2019.

[3] C. Chinedu Anyaoku, S. N. Bhattacharya, and R. Parthasarathy, "A novel methodology for measuring batch settling velocities of particles using Electrical Resistance Tomography," *Chemical Engineering Science*, vol. 250117364 pages, 2022.

[4] M. Mokhtari and J. Chaouki, "New technique for simultaneous measurement of the local solid and gas holdup by using optical fiber probes in the slurry bubble column," *Chemical Engineering Journal*, vol. 358, pp. 831–841, 2019.

[5] K. T. Aminu, D. McGlinchey, and A. Cowell, "Acoustic signal processing with robust machine learning algorithm for improved monitoring of particulate solid materials in a gas flowline," *Flow Measurement and Instrumentation*, vol. 65, pp. 33–44, 2019.

[6] Y. Yan, "Mass flow measurement of bulk solids in pneumatic pipelines," *Measurement Science and Technology*, vol. 7, no. 12, pp. 1687–1706, 1996.

[7] S. J. Tallon and C. E. Davies, "The effect of pipeline location on acoustic measurement of gas–solid pipeline flow," *Flow Measurement and Instrumentation*, vol. 11, no. 3, pp. 165–169, 2000.

[8] K. Albion, L. Briens, C. Briens, and F. Berruti, "Flow regime determination in horizontal pneumatic transport of fine powders using non-intrusive acoustic probes," *Powder Technology*, vol. 172, no. 3, pp. 157–166, 2007.

[9] Y. Zhou, L. Yang, Y. Lu, X. Hu, X. Luo, and H. Chen, "Flow regime identification in gas-solid two-phase fluidization via acoustic emission technique," *Chemical Engineering Journal*, vol. 334, pp. 1484–1492, 2018.

[10] P. J. Coghill, "Particle size determination by impact measurement in pneumatically conveyed solids," *Particle & Particle Systems Characterization*, vol. 18, no. 3, p. 114, 2001.

[11] R. K. Miller, A. A. Pollock, D. J. Watts, J. M. Carlyle, A. N. Tafuri, and J. J. Yezzi Jr, "A reference standard for the development of acoustic emission pipeline leak detection techniques," *NDT&E International*, vol. 32, pp. 1–8, 1999.

[12] A. Bastari, C. Cristalli, R. Morlacchi, and E. Pomponi, "Acoustic emissions for particle sizing of powders through signal processing techniques," *Mechanical Systems and Signal Processing*, vol. 25, no. 3, pp. 901–916, 2011.

[13] R. Hou, A. Hunt, R. A. Williams, and A. Hunt, "Acoustic monitoring of pipeline flows: particulate slurries," *Powder Technology*, vol. 106, no. 1-2, pp. 30–36, 1999.

[14] P. Zhang, Y. Yang, Z. Huang et al., "Machine learning assisted measurement of solid mass flow rate in horizontal pneumatic conveying by acoustic emission detection," *Chemical Engineering Science*, vol. 229116083 pages, 2021.

[15] J. W. R. oyd and J. Varley, "The uses of passive measuremen of acoustic emissions from chemical engineering processes," *Chemical Engineering Science*, vol. 56, pp. 1749–1767, 2001.

[16] C. Ren, J. Wang, and Y. Yang, "Signal analysis and judgement of acoustic emission of particle motion in gas-solid fluidized bed," *Science in China, Series B: Chemistry*, vol. 38, pp. 645–651, 2008.

[17] V. Rossbach, N. Padoin, H. F. Meier, and C. Soares, "Influence of acoustic waves on the solids dispersion in a gas-solid CFB riser: numerical analysis," *Powder Technology*, vol. 359, pp. 292–304, 2020.

[18] H. Sadegh, A. N. Mehdi, and A. Mehdi, "Classification of acoustic emission signals generated from journal bearing at different lubrication conditions based on wavelet analysis in combination with artificial neural network and genetic algorithm," *Tribology International*, vol. 95, pp. 426–434, 2016.

[19] E. M. Hansuld, L. Briens, A. Sayani, and J. A McCann, "An investigation of the relationship between acoustic emissions and particle size," *Powder Technology*, vol. 219, no. 3, pp. 111–117, 2012.

[20] A. Chakravarty and S. Misra, "Hydraulic fracture mapping using wavelet-based fusion of wave transmission and emission measurements," *Journal of Natural Gas Science and Engineering*, vol. 96, p. 104274, 2021.

[21] A. Mostafapour, S. Davoodi, and M. Ghareaghaji, "Acoustic emission source location in plates using wavelet analysis and cross time frequency spectrum," *Ultrasonics*, vol. 54, no. 8, pp. 2055–2062, 2014.

[22] O. Stankevych, V. Skalskyi, B. Klym, and P. Velykyi, "Identification of fracture mechanisms in cementitious composites using wavelet transform of acoustic emission signals," *Procedia Structural Integrity*, vol. 36, pp. 114–121, 2022.